Short Range 3D MIMO mmWave Channel Reconstruction via Geometry-aided AoA Estimation

Jarkko Kaleva†, Nitin Jonathan Myers*, Antti Tölli†, Robert W. Heath Jr.* and Upamanyu Madhow⋆

† *Centre for Wireless Communications, University of Oulu, Finland.*
* *Department of Electrical and Computer Engineering, The University of Texas at Austin, USA.*
⋆ *Department of Electrical and Computer Engineering, University of California at Santa Barbara, USA.*

***Abstract*—In some millimeter wave (mmWave) applications, such as wearables, the distance between the transceivers is relatively short. Further, the channel has significant angular spread in both azimuth and elevation domains even in line-of-sight (LoS). Under such conditions, hybrid mmWave architectures with multiple analog uniform planar arrays (UPAs) potentially allow spatial multiplexing even in LoS provided that the high rank structure of the channel is captured. The conventional far-field channel estimation methods are not generally suitable for these scenarios and perform poorly. We consider parametrized spatial channel estimation, where the known antenna array geometry is exploited to recover the angle-of-arrivals (AoAs) of the 3D multiple-input multiple-output (MIMO) channel. The channel is then reconstructed using these AoA estimates and the known geometry. We show that conventional maximum a posteriori (MAP) estimation of the channel parameters suffers from high computational complexity and may not be not applicable for low powered devices. To this end, we propose a lower complexity message passing algorithm for short range channel estimation. We show, by numerical examples, that the proposed technique achieves good performance with fewer pilot resources when compared to compressed sensing or antenna specific pilot based channel estimation.**

I. Introduction

MmWave systems enable the use of large antenna arrays in physically smaller devices. Such large arrays can be used to achieve narrow beams and better interference coordination. Typical mmWave systems, however, have fewer radio frequency chains than antennas to reduce the power consumption [1]. The subarray-based hybrid beamforming architecture is one example where a group of antennas share the same radio frequency chain. Hybrid mmWave architectures allow spatial multiplexing of parallel data streams to achieve better rates unlike plain analog beamforming-based systems and are already used, e.g., in the IEEE 802.11ay standard [2].

Hybrid architectures are useful in short range line-of-sight (LoS) scenarios, where the distance between the transmitting and receiving radios is comparable to the size of the antenna arrays. Some short range applications include communications in wearable networks and very high capacity wireless links, e.g., between servers in data centers [3]. In short range LoS scenarios, the rank of the multiple-input multiple-output (MIMO) channel can be larger than one. As a result, such channels allow spatial multiplexing unlike far field LoS channels, which have a rank one structure.

Short range channels exhibit special properties in LoS settings. Although the short range MIMO channel can have a high rank, it can be represented using fewer geometrical parameters. For example, channel matrices can be constructed from the distance between the transceivers and the relative orientation of the antenna arrays. The parametric structure in short range channels can be leveraged by channel estimation algorithms to reduce the number of pilot transmissions. Prior work on short range channel estimation has exploited such a parametric structure through geometry-aided message passing [4], [5]. The techniques proposed there estimate the geometrical angle-of-arrivals (AoAs), which are defined for small sections of the antenna array. The algorithms in [4] and [5], however, assume that the distribution of the distance between the transceivers is known. Furthermore, these solutions are limited to linear array-based systems.

In this paper, we develop a message passing-based short range channel estimation technique that does not require any knowledge on the distance distribution. The proposed method parameterizes the channel in planar array-based short range systems using 2D-AoA, i.e., the azimuth and elevation angles, at each subarray. Then, the 2D-AoAs associated with multiple subarrays are jointly estimated by exploiting the geometrical dependencies in the 2D-AoAs together with the channel measurements. The 2D-AoA estimates are then used to reconstruct the short range channel.

II. Short Range System Model

We consider a MIMO system with N_{rx} antennas at the receiver (RX). A subarray-based hybrid beamforming architecture [1] is considered at the RX. We assume N_{rf} RF chains at the RX; each RF chain at the RX is associated with a subarray. Every subarray at the RX employs a half-wavelength spaced uniform planar array with $N = N_{\mathrm{rx}}/N_{\mathrm{rf}}$ antennas. The centers of the subarrays at the RX are assumed to be collinear. The subarrays at the RX are equipped with an analog beamforming architecture with q-bit phase shifters. The phase shift alphabet is defined as $\mathbb{Q} = \{e^{\mathrm{j}2\pi k/2^q}/\sqrt{N} : k \in \{1, 2, 3, .., 2^q\}\}$. For simplicity, we assume that the transmitter (TX) is equipped with a uniform linear array (ULA) with N_{tx} antennas. Furthermore, a fully digital architecture is assumed at the TX. The fully digital architecture assumption allows a straightforward extension of our algorithm to UPA or any

other array geometry. Extending our algorithm to UPAs with a beamforming architecture at the TX is an interesting research direction. An illustration of the MIMO system considered in this paper is shown in Fig. 1.

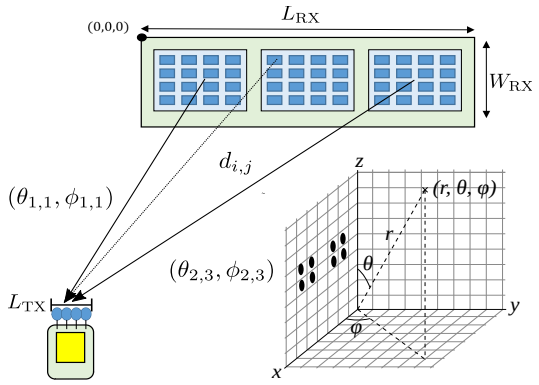

Fig. 1. Example of the MIMO system considered in this paper for $N_{\mathrm{rf}} = 3$ subarrays at the RX. Here, each RX subarray consists of a 4×4 UPA, i.e., $N = 16$, while the TX is equipped with $N_{\mathrm{tx}} = 4$ antennas.

Now, we explain the assumed short range LoS channel model. The length of the transmit array is defined as L_{tx}. The dimensions of the receive array is $W_{\mathrm{rx}} \times L_{\mathrm{rx}}$, as shown in Fig. 1. We denote the carrier wavelength by λ. Although the subarrays at the RX are $\lambda/2$-spaced UPAs, the spacing between the adjacent subarrays can be larger than $\lambda/2$. The short range scenario arises when the transceiver distance is comparable to the length of the arrays. One example is when r is comparable to L_{rx}. We assume a narrowband system and define the short range LoS MIMO channel matrix as $\mathbf{H} \in \mathbb{C}^{N_{\mathrm{rx}} \times N_{\mathrm{tx}}}$. The $(i,j)^{\mathrm{th}}$ entry of the channel matrix $\mathbf{H}$ is then [6]

$$H(i,j) = \frac{\lambda}{2\pi d_{i,j}} e^{-\mathrm{j}2\pi d_{i,j}/\lambda}, \tag{1}$$

where $d_{i,j}$ denotes the distance between the i^{th} RX antenna and the j^{th} TX antenna. We define $\mathbf{h}_{i,k} \in \mathbb{C}^N$, a vector in $\mathbf{H}$, as the channel between the k^{th} subarray at the RX and the i^{th} TX antenna. The narrowband assumption on the MIMO channel is simplistic, but we leave the extension to more realistic wideband channels to future work.

We now explain the channel measurement model in the uplink of the MIMO system. Let $t_\ell[m] \in \mathbb{C}$ be the pilot transmitted by the TX in the m^{th} training slot. In the same slot, the RX applies receive beamformer $\mathbf{w}_k[m] \in \mathbb{Q}^N$ to its k^{th} subarray to acquire the channel measurement $y_k[m]$. The conjugate transpose of $\mathbf{w}_k[m]$ is defined as $\mathbf{w}_k^*[m]$. Under a perfect synchronization assumption, the channel measurement $y_k[m]$ can be given as

$$y_k[m] = \mathbf{w}_k^*[m] \sum_{i=1}^{N_{\mathrm{rf}}} \mathbf{h}_{i,k} t_i[m] + v_k[m], \tag{2}$$

where $v_k[m] \sim \mathcal{N}_{\mathrm{c}}(0, \sigma^2)$ is circularly symmetric Gaussian noise with zero mean and variance σ^2. As $\mathbf{H}$ has $N_{\mathrm{rx}} N_{\mathrm{tx}}$ entries and the RX can acquire N_{rf} channel measurements in parallel, standard channel estimation requires a training overhead of $\mathcal{O}(N_{\mathrm{rx}} N_{\mathrm{tx}}/N_{\mathrm{rf}})$. In this paper, we show that a reasonable approximation of $\mathbf{H}$ can be estimated with fewer pilot transmissions when compared to $\mathcal{O}(N_{\mathrm{rx}} N_{\mathrm{tx}}/N_{\mathrm{rf}})$. The key idea underlying our approach is that the far-field assumption is more likely to be valid for a section of the antenna array rather than the full array [5]. Under this assumption, the subarray specific channels have a rank one structure. The rank of the full channel matrix $\mathbf{H}$, however, may be greater than one.

Due to the rank one assumption on the channel matrices corresponding to subarrays, we define the concept of local AoA for each subarray. A local AoA is simply the AoA defined for a subarray. Let $\theta_{i,k}$ and $\phi_{i,k}$ denote the elevation and the azimuth angles of arrival between the ray joining the i^{th} TX antenna and the midpoint of the k^{th} receive subarray, with the normal of the receive array. The angle pair $\theta_{i,k}$ and $\phi_{i,k}$ is called a local AoA. Due to the rank-one assumption on subarray specific channels, the AoAs within any receive subarray are considered to be invariant, and can be approximated to a local AoA. The AoAs can vary significantly across different RX subarrays. We denote $\theta_{i,k}$ and $\phi_{i,k}$ as a realization of a random variables $\Theta_{i,k}$ and $\Phi_{i,k}$, respectively. Further, we propose an algorithm to estimate the local AoAs from the channel measurements, while exploiting the dependencies among $\{(\theta_{i,k}, \phi_{i,k})\}_{k=1}^{N_{\mathrm{rf}}}$.

A. Channel measurement

The m^{th} pilot measurement for i^{th} TX antenna at the k^{th} receive subarray is

$$y_{i,k}[m] = \mathbf{w}_k^*[m] \mathbf{h}_{i,k} + v_k[m]. \tag{3}$$

We define a Vandermonde vector for a UPA subarray of size $N_{\mathrm{el}} \times N_{\mathrm{az}}$ as [7]

$$\mathbf{a}_N(\theta,\phi) = [1, \cdots, e^{-\mathrm{j}\pi(n_{\mathrm{el}}\sin(\theta)\cos(\phi) + n_{\mathrm{az}}\sin(\phi))}, \cdots, e^{-\mathrm{j}\pi((N_{\mathrm{az}}-1)\sin(\theta)\cos(\phi) + (N_{\mathrm{el}}-1)\sin(\phi))}]^T. \tag{4}$$

Note that $N = N_{\mathrm{az}} N_{\mathrm{el}}$. Under the far field assumption for subchannels, $\mathbf{h}_{i,k}$ can be approximated as $\alpha_k \mathbf{a}_N(\theta_{i,k}, \phi_{i,k})$, where $\alpha_{i,k}$ is an unknown complex gain. The measurement corresponding to the LOS path of $\mathbf{h}_{i,k}$ of $y_{i,k}[m]$ in (3) can be given as

$$y_{i,k}[m] = \alpha_{i,k} \mathbf{w}_k^*[m] \mathbf{a}_N(\theta_{i,k}, \phi_{i,k}) + v_k[m]. \tag{5}$$

Using M channel measurements over receive beam training vectors $\{\mathbf{w}_k[m]\}_{m=1}^M$, we obtain M projections of $\mathbf{a}_N(\theta_{i,k}, \phi_{i,k})$. These are defined as $\mathbf{y}_{i,k} \in \mathbb{C}^M$. Further, we can write (5) in a more condensed form as

$$\tilde{\mathbf{y}}_{i,k} = \alpha_{i,k} \mathbf{A}_k \mathbf{a}_N(\theta_{i,k}, \phi_{i,k}) + \mathbf{v}_k, \tag{6}$$

where the m^{th} row of $\mathbf{A}_k$ is $\mathbf{A}_k(m,:) = \mathbf{w}_k^*[m]$.

The first $M-1$ beam training vectors, i.e., $\{\mathbf{w}_k[m]\}_{m=1}^{M-1}$, are chosen as $M-1$ distinct random circulant shifts of $\mathbf{z}_{\mathrm{rx},k}$. The vector $\mathbf{w}_k[M]$ is defined as $\mathbf{w}_k[M] = \mathbf{w}_k[1] \odot [1, -1, -1, ..-1]^T$, where $\odot$ denotes the element-wise product. The M^{th} measurement is defined differently so that the unknown gain $\alpha_{i,k}$ can be estimated. With $\eta_{i,k}$ defined as

the first entry of $\mathbf{w}_k[1]$, it can be observed from (5) that $y_{i,k}[1] + y_{i,k}[M]$ is a noisy version of $2\alpha_{i,k}\eta_{i,k}$. An estimate of $\alpha_{i,k}$ is then $\hat{\alpha}_{i,k} = (y_{i,k}[1] + y_{i,k}[M])/2\eta_{i,k}$. Given the common phase estimate $\alpha_{i,k}$, we can write *phase normalized* received signal as $\mathbf{y}_{i,k} = \tilde{\mathbf{y}}_{i,k}/\alpha_{i,k}$.

We ignore the errors in estimating $\alpha_{i,k}$ to conclude that $\mathbf{y}_{i,k}$ is a realization of $\mathcal{N}_{\mathrm{c}}(\mathbf{A}_k\mathbf{a}_N(\theta_{i,k},\phi_{i,k}), \sigma^2\mathbf{I}/|\hat{\alpha}_{i,k}|^2)$. Thus, the scaled likelihood function $p(\mathbf{y}_{i,k}|\theta_{i,k},\phi_{i,k})$ is given by

$$p(\mathbf{y}_{i,k}|(\theta_{i,k},\phi_{i,k})) = e^{-|\hat{\alpha}_{i,k}|^2\|\mathbf{y}_{i,k}-\mathbf{A}_k\mathbf{a}_N(\theta_{i,k},\phi_{i,k})\|^2/\sigma^2}. \quad (7)$$

The maximum likelihood (MLE) of $\theta_{i,k}$ and $\phi_{i,k}$ can be obtained by maximizing $p(\mathbf{y}_{i,k}|(\theta_{i,k},\phi_{i,k}))$ in (7).

B. Geometric dependency of the local AoAs

In this section, we derive the geometric dependency between the local AoAs. This dependency arises due to the structure in short range channels. For example, given $(\theta_{i,1},\phi_{i,1})$ and $(\theta_{i,2},\phi_{i,2})$, the rest of the angles $(\theta_{i,k},\phi_{i,k}), k \notin \{1,2\}$ are deterministic. That is, there exists a feasible set of local AoAs that satisfies the geometric conditions given by structure of the antenna arrays. Let $\mathbf{n}$ denote the normal of the k^{th} RX subarray. Using relative coordinates where UPA array spans across the x and z axes, $\mathbf{n} = [0\ 1\ 0]^T$. Then, a normalized vector $\mathbf{z}_{i,1}$ towards $(\theta_{i,1},\phi_{i,1})$ can be given by

$$\mathbf{z}_{i,1} = \tilde{\mathbf{z}}_{i,1}/\|\tilde{\mathbf{z}}_{i,1}\|, \tilde{\mathbf{z}}_{i,1} = \mathbf{V}(\theta_{i,1},\phi_{i,1})\mathbf{n}, \quad (8)$$

where $\mathbf{V}(\theta_{i,1},\phi_{i,1}) =$

$$\begin{bmatrix}\cos(\theta_{i,1}) & -\sin(\theta_{i,1}) & 0\\ \sin(\theta_{i,1}) & \cos(\theta_{i,1}) & 0\\ 0 & 0 & 1\end{bmatrix}\begin{bmatrix}1 & 0 & 0\\ 0 & \cos(\phi_{i,1}) & -\sin(\phi_{i,1})\\ 0 & \sin(\phi_{i,1}) & \cos(\phi_{i,1})\end{bmatrix}.$$

The direction towards the second subarray $\mathbf{z}_{i,2}$ is given by (8). Then, the location of the signal source can be solved as

$$d_1\mathbf{z}_{i,1} + \mathbf{l}_1 = d_2\mathbf{z}_{i,2} + \mathbf{l}_2, \quad (9)$$

where d_1 and d_2 denote the signal source distance from the first and second subarray, respectively, and $\mathbf{l}_k$ is the relative coordinate of the k^{th} RX subarray. Now, the coordinates of the signal source are given by

$$\mathbf{s}_i = \mathbf{d}(1)\mathbf{z}_{i,1}, \quad (10)$$

where $\mathbf{d} = ([\mathbf{z}_{i,1}, -\mathbf{z}_{i,2}])^{-1}(-\mathbf{l}_1 + \mathbf{l}_2)$. Then, the direction vectors towards the signal source can be devised for each subarray k as $\mathbf{z}_{i,k} = \mathbf{s}_i - \mathbf{l}_k/\|\mathbf{s}_i - \mathbf{l}_k\|$.

The array geometry gives a prior joint distribution of feasible AoAs which is defined as

$$\bar{g}(\{\theta_{i,k},\phi_{i,k}\}_{k=1}^{N_{\mathrm{RF}}}) = \begin{cases}1, \{\theta_{i,k},\phi_{i,k}\}_{k=1}^{N_{\mathrm{RF}}} \text{ intersect at a point}\\ 0, \text{ otherwise.}\end{cases} \quad (11)$$

Furthermore, the known array geometry determines any local AoA based on the AoAs from any other two. Thus, we can formulate the scaled conditional distribution from subsequent arrays as in (12). It should be noted that solving the signal source from (10) based on estimated $\{\theta_k,\phi_k\}_{k=1}^{N_{\mathrm{RF}}}$ requires that $\bar{g}(\{\theta_k,\phi_k\}_{k=1}^{N_{\mathrm{RF}}}) = 1$. Unlike in [4], [5], where only ULAs were considered, the MLE that independently maximizes (7) over $\{(\theta_{i,k},\phi_{i,k})\}_{k=1}^{N_{\mathrm{rf}}}$ and does not exploit such dependency is not applicable, and hence, the independent estimates are unlikely to satisfy the feasibility condition $\bar{g}(\{\theta_k,\phi_k\}_{k=1}^{N_{\mathrm{RF}}}) = 1$. Thus, it is imperative to device algorithms that exploit the geometric structure to ensure feasible local AoA estimates over the RX subarrays.

C. Channel reconstruction

As shown in Section II-B, the signal source deduced based on the known local AoAs. Furthermore, knowing the antenna coordinates and (1), we can reconstruct the corresponding LoS MIMO channel.

To begin with, we assume that the RX has knowledge of, both, the TX and RX antenna array geometries and can compute the position of all the RX antenna elements relative to a common reference. As shown in (10), the RX can compute the position vectors of the first and $N_{\mathrm{rf}}{}^{\mathrm{th}}$ TX subarrays as $\mathbf{s}_1$ and $\mathbf{s}_{N_{\mathrm{rf}}}$, respectively. Knowing these coordinates and the known TX geometry, the RX can accurately calculate the antenna element coordinates and construct the LoS MIMO channel, solely based on the geometry information and local AoA estimates. Essentially, the RX estimates the location of the two ends (first/last antenna) of the TX ULA and interpolates all TX antenna locations between the two estimated ULA antenna locations using the known TX geometry.

III. Geometry-aided AoA estimation using MAP

As shown in Section II, the short range LoS MIMO channel between sufficiently small subarrays can be parametrized via the known common phase and AoAs. In this section, we model the AoA estimation as joint MAP estimation using a set of beam training measurements. Here, we focus on estimating the local AoAs between the i^{th} TX array and all $k = 1,\ldots,N_{\mathrm{rf}}$ RX subarrays. The same process can be done in parallel for all TX arrays as they employ pilot sequences to distinguish the TX subarrays.

The MAP estimate for the i^{th} TX array can be given as

$$\begin{aligned}\underset{(\theta_{i,k},\phi_{i,k})}{\arg\max}\quad & f_{\mathsf{map}}(\{(\theta_{i,k},\phi_{i,k})\}_{k=1}^{N_{\mathrm{rf}}})\\ \text{s.t.}\quad & (\theta_{i,k},\phi_{i,k}) \in \mathcal{A}, k = 1,\ldots,N_{\mathrm{rf}},\end{aligned} \quad (13)$$

where we denote a set of azimuth/elevation angle pairs as $\mathcal{A} = \{(\theta,\phi)|\theta \in [-\pi/2,\pi/2], \phi \in [-\pi/2,\pi/2]\}$. The objective function is given as

$$\begin{aligned}&f_{\mathsf{map}}(\{(\theta_{i,k},\phi_{i,k})\}_{k=1}^{N_{\mathrm{rf}}}) =\\ &p(\mathbf{y}_{i,k}|\{(\theta_{i,k},\phi_{i,k})\}_{k=1}^{N_{\mathrm{rf}}})\bar{g}(\{(\theta_{i,k},\phi_{i,k})\}_{k=1}^{N_{\mathrm{rf}}}) =\\ &\textstyle\prod_{k=1}^{N_{\mathrm{rf}}} p(\mathbf{y}_{i,k}|(\theta_{i,k},\phi_{i,k}))\bar{g}(\{(\theta_{i,k},\phi_{i,k})\}_{k=1}^{N_{\mathrm{rf}}}),\end{aligned} \quad (14)$$

where the final step follows from the independent measurements. The downside of the MAP estimation is the inherent complexity due to the large search space, where the dimensions are given by $\{(\theta_{i,k},\phi_{i,k})\}_{k=1}^{N_{\mathrm{rf}}} \in \mathcal{A}^{N_{\mathrm{rf}}}$. The complexity of the standard MAP algorithm increases exponentially with the number of RF chains. To this end, in the sequel, we provide a low complexity message passing algorithm akin to the one described in [4], [5] for ULA systems.

$$g(\theta_{i,k},\phi_{i,k}|\theta_{i,k-1},\phi_{i,k-1},\theta_{i,k-2},\phi_{i,k-2}) = \begin{cases} p(\theta_{i,k-1},\phi_{i,k-1})p(\theta_{i,k-2},\phi_{i,k-2}), \text{ if } (\theta_{i,k-1},\phi_{i,k-1}) \text{ and } (\theta_{i,k-2},\phi_{i,k-2}) \\ \quad \text{intersect at a point} \\ 0, \text{ otherwise.} \end{cases} \tag{12}$$

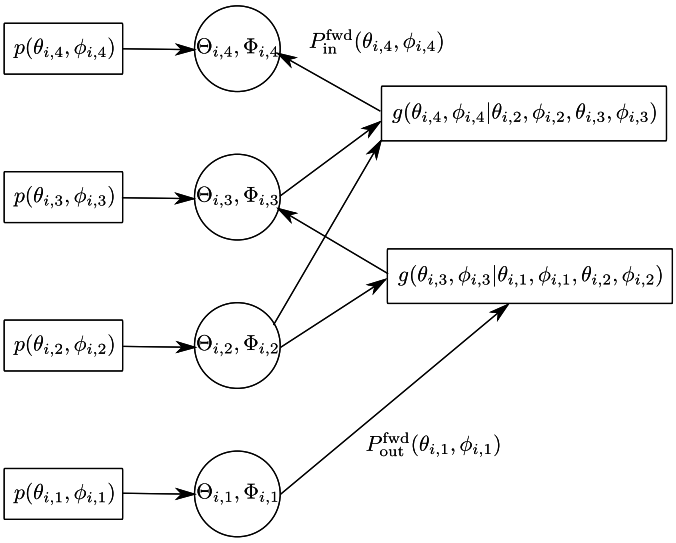

Fig. 2. Factor graph for forward and backward passes in geometry-aided message passing. The random variable $\Theta_{i,k}$ models a realization of $\theta_{i,k}$.

IV. Geometry-aided MP for AoA estimation

We aim to decrease the computational complexity of the MAP method by using a message passing algorithm that simultaneously exploits the local AoA likelihood and the prior distribution of feasible angles. A message flow out of a node models a distribution of the corresponding random variable. Fig. 2 illustrates the message flow graph. These messages are exchanged among the circular and rectangular nodes to estimate $\{(\theta_{i,k},\phi_{i,k})\}_{k=1}^{N_{\text{rf}}}$. There are two phases. In the forward pass, messages flow sequentially among $\{(\Theta_{i,k},\Phi_{i,k})\}_{k=1}^{N_{\text{rf}}}$. In the backward pass the message flows is in the opposite direction. The messages in both directions are computed using the sum-product algorithm [8].

We begin explaining the algorithm by considering the forward pass likelihood $p(\theta_{i,1},\phi_{i,1})$. This is directed to node $(\Theta_{i,1},\Phi_{i,1})$ that passes $p(\theta_{i,1},\phi_{i,1})$ to the geometry factors $g(\theta_{i,3},\phi_{i,3}|\theta_{i,1},\phi_{i,1},\theta_{i,2},\phi_{i,2})$. We define the output likelihood as $P_{\text{out}}^{\text{fwd}}(\theta_{i,1},\phi_{i,1}) = p(\theta_{i,1},\phi_{i,1})$. The geometry factor provides outflow for node $(\Theta_{i,1},\Phi_{i,1})$ as $P_{\text{out}}^{\text{fwd}}(\theta_{i,1},\phi_{i,1})$. Furthermore, it contains the conditional distribution $g(\theta_{i,3},\phi_{i,3}|\theta_{i,1},\phi_{i,1},\theta_{i,2},\phi_{i,2})$. Finally, using the two functions, the geometry factor passes the message $P_{\text{in}}^{\text{fwd}}(\theta_{i,3},\theta_{i,3})$ to $(\Theta_{i,3},\Phi_{i,3})$ in (15). As in [4], we can interpret (15) as a belief about $(\Theta_{i,3},\Phi_{i,3})$. This is a scaled probability distribution of $\Theta_{i,3}$ and $\Phi_{i,3}$ as believed by the geometry factor with information about $(\Theta_{i,1},\Phi_{i,1},\Theta_{i,2},\Phi_{i,2})$. Furthermore, the inflow $P_{\text{in}}^{\text{fwd}}(\theta_{i,3},\phi_{i,3})$ contains information about $(\Theta_{i,3},\Phi_{i,3})$, which is independent of the measurements acquired by the corresponding subarray. Node $(\Theta_{i,3},\Theta_{i,3})$ combines the channel measurements $p(\theta_{i,3},\phi_{i,3})$ and $P_{\text{in}}^{\text{fwd}}(\theta_{i,3},\phi_{i,3})$ as $P_{\text{out}}^{\text{fwd}}(\theta_{i,3},\phi_{i,3}) = p(\theta_{i,3},\phi_{i,3})P_{\text{in}}^{\text{fwd}}(\theta_{i,3},\phi_{i,3})$, which is sent to the factors with $g(\theta_{i,4},\phi_{i,4}|\theta_{i,3},\phi_{i,3},\theta_{i,2},\phi_{i,2})$. Here, $P_{\text{in}}^{\text{fwd}}(\theta_{i,4},\phi_{i,4})$ and $p(\theta_{i,4},\phi_{i,4})$ accumulate belief about $\Theta_{i,4}$ and $\Phi_{i,4}$ with $g(\theta_{i,4},\phi_{i,4}|\theta_{i,3},\phi_{i,3},\theta_{i,2},\phi_{i,2})$, $P_{\text{out}}^{\text{fwd}}(\theta_{i,3},\phi_{i,3})$ and $P_{\text{out}}^{\text{fwd}}(\theta_{i,2},\phi_{i,2})$. The incoming messages to each $(\theta_{i,k},\phi_{i,k})$, i.e., $P_{\text{in}}^{\text{fwd}}(\theta_{i,3},\phi_{i,3})$, are computed using an expression similar to (15). This is repeated until the final ${N_{\text{rf}}}^{\text{th}}$ node is reached.

As the forward pass ends with the ${N_{\text{rf}}}^{\text{th}}$ node, it does not exploit information about $\{\theta_{i,n},\phi_{i,n}\}_{n=k}^{N_{\text{rf}}}$ to provide information about $(\theta_{i,k-1},\phi_{i,k-1})$. Similarly to [4], [5], we define a backward pass to additional exploit the information provided by the ${N_{\text{rf}}}^{\text{th}}$ node. In the backward pass, the messages flow in the opposite direction. That is, the message from node $(\Theta_{i,N_{\text{rf}}},\Phi_{i,N_{\text{rf}}})$, i.e., $P_{\text{out}}^{\text{bkd}}(\theta_{i,N_{\text{rf}}},\phi_{i,N_{\text{rf}}}) = p(\theta_{i,N_{\text{rf}}},\phi_{i,N_{\text{rf}}})$, flows into the geometry factor with $g(\theta_{N_{\text{rf}}-2},\phi_{N_{\text{rf}}-2}|\theta_{i,N_{\text{rf}}},\phi_{i,N_{\text{rf}}},\theta_{i,N_{\text{rf}}-1},\phi_{i,N_{\text{rf}}-1})$. This factor provides belief of $(\theta_{i,N_{\text{rf}}-2},\phi_{i,N_{\text{rf}}-2})$ as $p_{\text{in}}^{\text{bkd}}(\theta_{i,N_{\text{rf}}-2},\phi_{i,N_{\text{rf}}-2})$. The belief is supported by $p(\theta_{i,N_{\text{rf}}},\phi_{i,N_{\text{rf}}})$ and $p(\theta_{i,N_{\text{rf}}-1},\phi_{i,N_{\text{rf}}-1})$. As in the forward pass, backward pass messages are computed by (16) and $P_{\text{out}}^{\text{bkd}}(\theta_k,\phi_k) = p(\theta_k,\phi_k)P_{\text{in}}^{\text{bkd}}(\theta_k,\phi k)$.

In the forward and backward passes, the first and last node do not have any inflow of side information from earlier nodes in the chain. For the sake of generality we set $P_{\text{in}}^{\text{fwd}}(\theta_{i,1},\phi_{i,1}) = \mathcal{U}(\theta_{i,1},\phi_{i,1})$ and $P_{\text{in}}^{\text{bkd}}(\theta_{i,N_{\text{rf}}},\phi_{i,N_{\text{rf}}}) = \mathcal{U}(\theta_{i,N_{\text{rf}}},\phi_{i,N_{\text{rf}}})$, where $\mathcal{U}(\theta,\phi)$ denotes a uniform distribution over θ and ϕ.

Each node in the message passing graph $(\Theta_{i,k},\Phi_{i,k})$ always receives information from $P_{\text{in}}^{\text{fwd}}(\theta_{i,k},\phi_{i,k})$ and $P_{\text{in}}^{\text{bkd}}(\theta_{i,k},\phi_{i,k})$. In addition, they exploit the local AoA likelihoods $p(\theta_{i,k},\phi_{i,k})$. This last step combines these three sources of information regarding $\Theta_{i,k}$ and $\Phi_{i,k}$ in distribution

$$p_{\text{gmp}}(\theta_{i,k},\phi_{i,k}) = p(\theta_{i,k},\phi_{i,k})P_{\text{in}}^{\text{fwd}}(\theta_{i,k},\phi_{i,k})P_{\text{in}}^{\text{bkd}}(\theta_{i,k},\phi_{i,k}). \tag{17}$$

The final estimate of $(\theta_{i,k},\phi_{i,k})$ is the maximizer of (17).

The integrals, for e.g. in (15), are implemented using a discrete sum with given partitioning resolution δ. Similarly, the search for the MAP (14), is done be over a grid with resolution δ. The grid search complexity is $\mathcal{O}((2\pi/\delta)^{N_{\text{rf}}})$, while the MP complexity is $\mathcal{O}((N_{\text{rf}}-2)(2\pi/\delta)^2)$

V. Numerical examples

In our numerical examples, we consider $N_{\text{rf}} = 4$ UPA subarrays with 4×4 in each subarry at the RX. The TX

$$P_{\text{in}}^{\text{fwd}}(\theta_{i,3},\phi_{i,3}) = \int_{\mathcal{A}}\int_{\mathcal{A}} P_{\text{out}}^{\text{fwd}}(\theta_{i,1},\phi_{i,1}) P_{\text{out}}^{\text{fwd}}(\theta_{i,2},\phi_{i,2}) g(\theta_{i,3},\phi_{i,3}|\theta_{i,1},\phi_{i,1},\theta_{i,2},\phi_{i,2})\, d(\theta_{i,1},\phi_{i,1},\theta_{i,2},\phi_{i,2}) \tag{15}$$

$$P_{\text{in}}^{\text{bkd}}(\theta_{i,k-2},\phi_{i,k-2}) = \int_{\mathcal{A}}\int_{\mathcal{A}} P_{\text{out}}^{\text{bkd}}(\theta_{i,k},\phi_{i,k}) P_{\text{out}}^{\text{bkd}}(\theta_{i,k-1},\phi_{i,k-1}) g(\theta_{i,k-2},\phi_{i,k-2}|\theta_{i,k},\phi_{i,k},\theta_{i,k-1},\phi_{i,k-1}) \, d(\theta_{i,k},\phi_{i,k},\theta_{i,k-1},\phi_{i,k-1}) \tag{16}$$

has fully digital $N_{\text{tx}} = 4$ ULA antenna array with $N_{\text{rf}} = 4$ RF chains. The subarrays are colinear. The mmWave carrier frequency is set to 60GHz, which corresponds to $\lambda = 5\,\text{mm}$. The receive SNR is set to 5 dB. We have used the MIMO indoor channel model proposed in [6]. This model incorporates the LOS channel with reflections from the ceiling, side-walls, and the floor to simulate more realistic fading scenario. Note that our algorithm only recovers the LOS channel component. The distance between the TX and RX is limited to be within $[20\text{cm}, 120\text{cm}]$, which complies with typical wearables scenario. As a reference, we compare our methods to DFT-based beam training, where $M = N_{\text{tx}}$ beams w_k are chosen from a DFT codebook [4].

The length of the arrays at the TX and the RX are $L_{\text{tx}} = 4\,\text{cm}$ and $L_{\text{rx}} = 18\,\text{cm}$. This simulates, for instance, a scenario where the RX array is mounted on a augmented reality headset, and the TX array is a smart watch. The spacing between the midpoint of successive receive subarrays is $5.75\,\text{cm}$, and the spacing between neighbouring transmit antennas is $1.33\,\text{cm}$. The TX and RX arrays are placed on a horizontal plane at a height of $1.5\,\text{m}$, in a room of dimensions $5\,\text{m} \times 5\,\text{m} \times 3\,\text{m}$. The orientations of the TX and RX arrays are chosen at random. The constant gap between the proposed schemes and perfect CSI are caused by the NLOS channel components and accuracy of the common phase estimate $\alpha_{i,k}$ in (5).

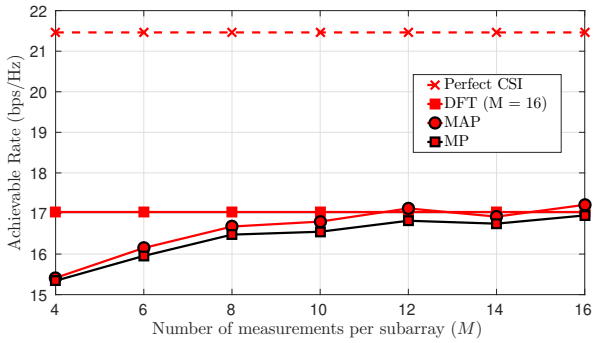

Fig. 3. Achievable rate with number of beam sweeps (M).

Fig 3 shows that the proposed algorithms achieve the performance of the DFT method [4], when the number of measurements is above $M = 6$. However, even with $M = 4$, we have achieved significant gain. This illustrates that we can significantly reduce the amount of training for channel acquisition by properly exploiting the array geometry.

VI. Conclusions and Future Work

We introduced novel channel reconstruction methods based on 3D AoA estimation, particularly aimed for short range devices, such as, wearables. The proposed algorithms were able to reconstruct the LoS MIMO channel with greatly reduced training when compared to conventional channel estimation. The proposed MP algorithm was shown to provide lower computational complexity with comparable performance with respect to the more complex MAP algorithm.

The method provided in this paper exploits the geometric information regarding the RX array in (11). It can be extended to geometric structure of the TX array as well, by considering simultaneously supporting estimation of multiple TX antennas and only considering AoAs there in that are supported by the known TX array geometry. In this paper, we have considered fully digital TX arrays. In the future, we will consider less complex hybrid architecture at TX, where the local AoA training over TX beamformers requires attention.

Aknowledgements

This research is supported by the Academy of Finland under grant numbers 311741 and 318927 (6Genesis Flagship), and by the U.S. National Science Foundation under grant numbers CNS-1702800 and ECCS-1711702.

References

[1] R. W. Heath, N. Gonzalez-Prelcic, S. Rangan, W. Roh, and A. M. Sayeed, "An overview of signal processing techniques for millimeter wave MIMO systems," *IEEE J. Sel. Topics Signal Process.*, vol. 10, no. 3, pp. 436–453, 2016.

[2] Y. Ghasempour, C. R. da Silva, C. Cordeiro, and E. W. Knightly, "IEEE 802.11 ay: Next-generation 60 GHz communication for 100 Gb/s Wi-Fi," *IEEE Commun. Mag.*, vol. 55, no. 12, pp. 186–192, 2017.

[3] J. Shin, E. G. Sirer, H. Weatherspoon, and D. Kirovski, "On the feasibility of completely wireless datacenters," in *2012 ACM/IEEE Symposium on Architectures for Networking and Communications Systems (ANCS)*, Oct 2012, pp. 3–14.

[4] J. Kaleva, N. J. Myers, A. Tölli, and R. W. Heath, "A geometry-aided message passing method for AoA-based short range MIMO channel estimation," in *20th IEEE International Workshop on Signal Processing Advances in Wireless Communications, SPAWC 2019, Cannes, France, July 2-5, 2019*.

[5] N. J. Myers, J. Kaleva, A. Tölli, and R. W. H. Jr., "Message passing-based link configuration in short range millimeter wave systems," 2019. [Online]. Available: http://arxiv.org/abs/1907.05009

[6] E. Torkildson, U. Madhow, and M. Rodwell, "Indoor millimeter wave MIMO: Feasibility and performance," *IEEE Trans. on Wireless Commun.*, vol. 10, no. 12, pp. 4150–4160, 2011.

[7] O. E. Ayach, S. Rajagopal, S. Abu-Surra, Z. Pi, and R. W. Heath, "Spatially sparse precoding in millimeter wave mimo systems," *IEEE Transactions on Wireless Communications*, vol. 13, no. 3, pp. 1499–1513, March 2014.

[8] F. R. Kschischang, B. J. Frey, H.-A. Loeliger *et al.*, "Factor graphs and the sum-product algorithm," *IEEE Trans. on Inform. theory*, vol. 47, no. 2, pp. 498–519, 2001.